Coordinated Launching of an Ornithopter with a Hexapedal Robot

Cameron J. Rose, Parsa Mahmoudieh, and Ronald S. Fearing

***Abstract*— In this work, we develop a cooperative launching system for a 13.2 gram ornithopter micro-aerial vehicle (MAV), the H^{2}Bird, by carrying it on the back of a 32 gram hexapedal millirobot, the VelociRoACH. We determine the necessary initial velocity and pitch angle for take off using force data collected in a wind tunnel and use the VelociRoACH to reach these initial conditions for successful launch. In the wind tunnel predicted success region, we were able to complete a successful launch for 75 percent of the 12 trials in that region.**

Although carrying the H^{2}Bird on top of the VelociRoACH at a stride frequency of 17 Hz increases our average power consumption by about 24.5 percent over solo running, the H^{2}Bird, in turn, provides stability advantages to the VelociRoACH. We observed that the variance in pitch and roll velocity with the H^{2}Bird is about 90 percent less than without. Additionally, with the H^{2}Bird flapping at 5 Hz during transport, we observed an increase of 12.7 percent of the steady state velocity. Lastly, we found that the costs of transport for carrying the H^{2}Bird flapping and without (6.6 and 6.8) are lower than the solo costs of transport for the VelociRoACH and for the H^{2}Bird (8.1 and 10.1).

I. INTRODUCTION

Bio-inspired millirobotic systems are a rapidly expanding research area with many applications in the medical, emergency services, and biological fields. In nature, animals have evolved many robust locomotion and sensing adaptations to suit their environments. Smaller animals, in particular, are generally more agile than larger animals because of their smaller moment of inertia and scaling trends of muscle fibers among small and large animals [1][2][3]. The study of these behaviors allows for the design and production of light-weight, inexpensive robotic systems that can be mass produced for a variety of applications.

While millirobots' size provides some advantages in terms of portability and transport; power, size, and weight constraints limit the actuation, processing power, sensing, and battery life that can be included on the system. These limitations can be mitigated by the use of robotic teams with varying specializations that enable the traversal of complex environments. In particular, a legged robot has advantages over wheeled and tank-tracked ground systems while traversing uneven terrain, through better control of ground reaction forces [4][5]. This ability to rapidly traverse uneven terrain has also been shown in nature for the Death-Head cockroach (*B. discoidalis*) [6]. While legged robots are great for uneven terrain, they have difficulty traversing tall obstacles.

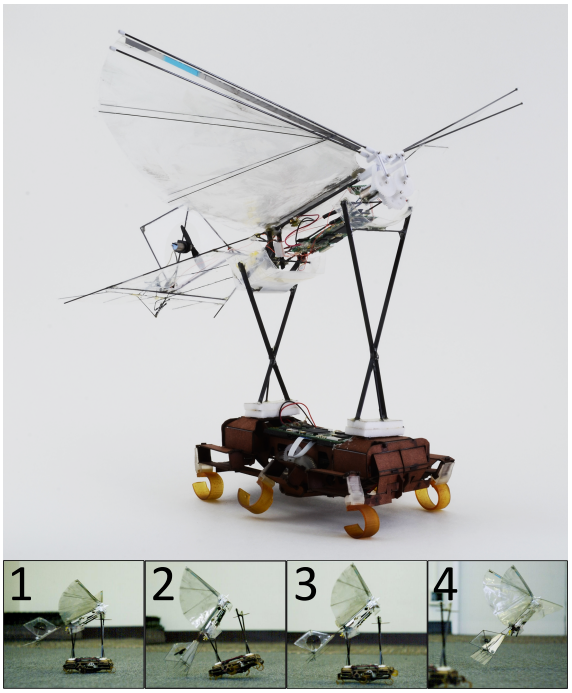

Fig. 1. VelociRoACH with cradle and H^{2}Bird ornithopter MAV (top), and launch sequence from left to right (bottom).

A flying millirobot has the ability to overcome tall obstacles and flapping-winged robots can have energy advantages over rotary and fixed wing fliers when it comes to mixed-modal flight (gliding, forward flight). Additionally, flapping flight may save aerodynamic power compared to steady flight at small scales [7]. At the same time, sub-15 gram fliers are limited in terms of battery life, actuation, and sensing due to aerodynamic constraints, which adversely affect maximum payload limits. The sole use of millirobotic fliers is impractical on missions with lengthy activity times because of battery life constraints. Therefore, cooperation of legged crawlers and flapping-winged fliers is warranted in applications such as exploring rough terrain.

Some researchers have pursued the design of robots that can traverse an environment using a variety of methods of locomotion. In particular, we are interested in a subset of these multi-modal robots that can navigate both terrestrial and aerial environments [8] [9]. Two such robots are the BOLT [10], designed by Peterson et. al, and the MALV II [11], by Bachmann et. al. Both robots use legs on the front of robotic fliers to overcome obstacles taller than the robot's height. Both robots can also transition from legged running

*This material is based upon work supported by the National Science Foundation under IGERT Grant No. IIS-0931463, and the United States Army Research Laboratory under the Micro Autonomous Science and Technology Collaborative Technology Alliance.

The authors are with the Department of Electrical Engineering and Computer Sciences, University of California, Berkeley, CA 94720 USA {c_rose, ronf}@eecs.berkeley.edu, parsa.m@berkeley.edu

to flying. The BOLT [10] uses small running legs to reach takeoff speed, but there is no way to run without flapping the wings, as the same motor drives both. Aerodynamic surfaces on legged robots can also provide benefits in terms of stability and running speed as demonstrated by Peterson et. al with Dash+ Wings [12] and Haldane et. al with the VelociRoACH [13]. In spite of these benefits and the versatility of multi-modal robots, it is difficult for multi-modal robots to excel at both modes with a single design, due to power and weight constraints.

In this paper we experiment with transporting and launching a flapping-winged robot, the H^{2}Bird [14], with a legged millirobot, the VelociRoACH [13]. The H^{2}Bird is designed specifically for flight, but is unable to take off from the ground from rest because the wings cannot provide enough thrust to counter its ground contact drag and weight. We determine the conditions required for takeoff experimentally in a wind tunnel. We then experimentally determine the conditions required in free flight, using a launch mechanism mounted on the top of the VelociRoACH. Finally, we determine the energy costs to bring the H^{2}Bird to the required velocity for takeoff and the potential effects on gait and stability for the VelociRoACH.

II. ROBOTIC PLATFORMS

We experimented with two robotic platforms: the VelociRoACH, designed specifically for terrestrial locomotion, and the H^{2}Bird, designed specifically for aerial locomotion.

A. VelociRoACH

The VelociRoACH [13] is a six-legged running robot weighing 30 grams (including 3.7 V, 120 mAh battery) that can run up to 2.7 m/s with a 24 Hz stride frequency. The VelociRoACH uses two 3.3 Ohm coreless, brushed DC motors in separate gear boxes for independently driving the legs, and magnetic Hall effect encoders to regulate the stride frequency and gait phase. On-board, the VelociRoACH has a micro-controller, the ImageProc 2.5[1], which holds a 40 MIPS microprocessor, 6 DOF IMU, IEEE 802.15.4 radio, and motor drivers.

B. H^{2}Bird Ornithopter

The H^{2}Bird [14] is a flapping-winged micro aerial vehicle (MAV) that weighs 13.2 grams and has a wing span of 26.5 cm. It has carbon fiber reinforced wings, frame, and tail and uses the i-Bird RC flier power train. The H^{2}Bird uses the ImageProc 2.4 controller, which is an earlier, lighter version of the VelociRoACH control board. Yaw and pitch control is computed on-board, with a tail-mounted propeller for yaw control and a servo driven elevator for pitch control. The H^{2}Bird can operate for about 2.5 minutes of flight time on a single 3.7 V, 90 mAh battery charge. The maximum flap frequency is approximately 16 Hz.

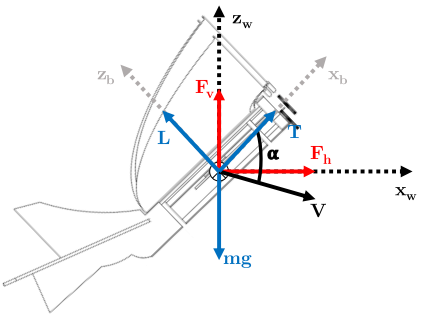

Fig. 2. Free body diagram for the H^{2}Bird.

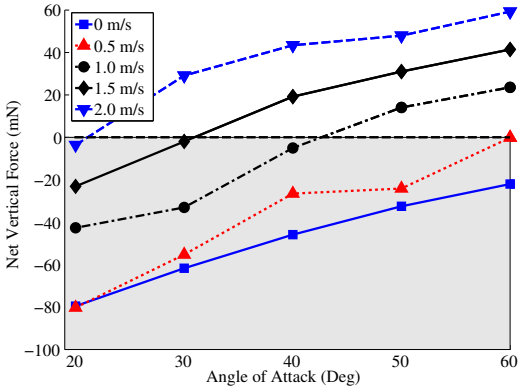

Fig. 3. Net lift over a range of angles of attack and wind speeds at 16 Hz flap speed. The dashed black line indicates the line of zero net vertical force. Above the line are feasible conditions for takeoff and infeasible conditions are below.

III. ROBOTIC BEHAVIORS AND CONTROL

To design the launching method used by the VelociRoACH to bring the H^{2}Bird up to takeoff initial conditions, the locomotive behaviors of both robots must be considered. These behaviors are dictated by both the physical actuation of the robots and the propulsion control scheme.

A. VelociRoACH Dynamic Behavior

The VelociRoACH's gear ratio is 16:1 allowing a 4-24 Hz range of stride frequencies. The separate gear boxes enable differential steering for each set of legs. The fore and aft legs of the VelociRoACH are mechanically constrained 180 degrees out of phase from the middle leg for an alternating tripod gait. For straight-line running, a software controller is used to enforce a 180 degree offset phase between the right and left sets of legs, such that the middle leg of one side steps simultaneously with the fore and aft legs of the other side. For our experiments, yaw control using angular position sensing and steering was not used (e.g. Pullin et. al [15]), so gait inconsistencies can result in yaw moments and deviations from straight running.

B. H^{2}Bird Ornithopter Dynamic Behavior

To determine the region of initial conditions in angle of attack and velocity for which the H^{2}Bird can take off, we

[1]ImageProc 2.5:
https://github.com/biomimetics/imageproc_pcb

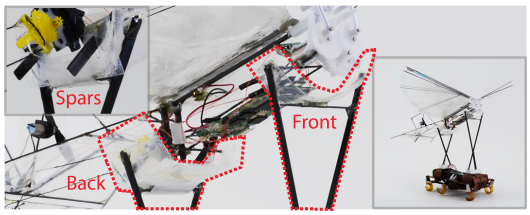

Fig. 4. The launch cradle on top of the VelociRoACH, highlighted by the red dashed line. The carbon fiber spars through the back of the cradle are shown in the top-left inset.

conducted experimental trials in a 45.5 cm x 45.5 cm x 91.5 cm wind tunnel [16]. The free body diagram in Figure 2 shows the distribution of relevant forces for the H^{2}Bird. In the free body diagram, T is the horizontal force in the H^{2}Bird frame, L is the vertical force in the H^{2}Bird frame, m is the mass, g is gravity, and α is the angle of attack. Using a 6DOF force and torque sensor we determined the total vertical force F_v in world coordinates. For each trial, we flapped the wings at the maximum speed of 16 Hz and measured the forces and moments for angles of attack from -60 to 90 degrees in 10 degree increments, and velocities from 0 to 2 m/s in 0.5 m/s increments. Using the force data, we computed the total vertical force, F_v, as follows:

$$F_v = T \sin \alpha + L \cos \alpha - mg \tag{1}$$

The results of the experiments are in Figure 3, where the dashed black line is the line of zero total vertical force. The operating points above the line are feasible takeoff conditions, and the operating points below the line are infeasible takeoff conditions. The aerodynamics of the H^{2}Bird and the differences between wind tunnel and free flight collected data sets are discussed further in [16].

It is important to note that the H^{2}Bird cannot produce enough lift to take off from the ground at rest. At 90 degrees pitch angle (sitting vertically, with all of the thrust in the upward direction), maximum flap speed, and zero velocity, the net vertical force ($T - mg$) on the H^{2}Bird is approximately -10 mN. This net force indicates that the weight of the H^{2}Bird is 10 mN larger than its maximum thrust. Therefore, the forward velocity provided by the VelociRoACH is necessary for takeoff.

C. Control and Launching

During our launching experiments, each robot uses its own control scheme and mechanisms to govern its individual motion.

The H^{2}Bird uses three PID controllers to control its pitch, yaw, and thrust. The pitch PID controller regulates the motion of the elevator mounted on the back of the tail and the yaw controller regulates the speed of a propeller mounted on the vertical stabilizer. The pitch and yaw controllers both use angular position estimates computed on-board by integrating the angular velocity measurements from the gyroscope. The thrust controller tracks a reference flap frequency using a Hall effect sensor mounted on one of the output gears on the wing gear box.

To bring the H^{2}Bird to a desired launch velocity, a rigidly mounted cradle, shown in Figure 4 with the front and back annotated, was affixed to the top of the VelociRoACH, with the front and back of the cradle 7 cm apart. The cradle is constructed of 2.5 mm by 1 mm flat carbon fiber spars for the support beams, and 2 mil PET for the sling in which the H^{2}Bird sits. The mount is constructed such that the H^{2}Bird sits at an angle of 25° in the cradle. This angle was selected to provide the H^{2}Bird with a high enough initial pitch angle for takeoff, and to minimize the drag on the VelociRoACH as much as possible. The VelociRoACH has a maximum running velocity of 2.7 m/s without the H^{2}Bird on top, and the minimum angle possible for takeoff at that speed is 18 degrees. Setting a cradle angle requiring the VelociRoACH to run at its maximum speed to take off is impractical, however, so we relaxed our velocity constraint by raising the cradle angle to 25°.

The cradle on the top of the VelociRoACH is 9 cm tall in the front and 6 cm tall in the back. We chose this height to prevent the tail of the H^{2}Bird from scraping the ground as it pitches up before it takes off.

To prevent the H^{2}Bird from sliding off of the cradle due to angular moments caused by the legs of the VelociRoACH making contact with the ground, we cut 5 mm x 1 mm slots in the back of the cradle at 25 mm apart, and affixed 2.5 mm by 1 mm flat carbon fiber spars to the back of the H^{2}Bird. These spars are depicted in the top left inset of Figure 4. We observed that without the rods, the H^{2}Bird tended to roll to the left or right and slide off of the cradle, so this modification constrains the rolling motion, thereby preventing the H^{2}Bird from falling out of the cradle. The slots also helped to minimize some of the initial pitch motion as the VelociRoACH initially accelerates.

A picture of the full system, with the H^{2}Bird sitting in the cradle on top of the VelociRoACH is in Figure 1.

IV. EXPERIMENTS AND RESULTS

We conducted experiments launching the H^{2}Bird from the cradle on top of the VelociRoACH to determine the feasibility and performance of the cooperative launch. We also investigated the effect that the H^{2}Bird has on the running performance of the VelociRoACH.

A. Cooperative Launching

To test our cooperative launching system, we conducted experiments by attempting to launch the H^{2}Bird under various conditions. Each trial consisted of the following steps, graphically depicted in the bottom portion of Figure 1:

1) The H^{2}Bird is placed in the cradle at an angle of 25° and the VelociRoACH is at rest.
2) The VelociRoACH begins running at a predetermined stride frequency and the H^{2}Bird pitches up initially due to the sudden forward acceleration.
3) The VelociRoACH reaches a steady state velocity and the H^{2}Bird reaches a steady state pitch angle.
4) The H^{2}Bird is given a launch command through a radio frequency (RF) link by the experimenter shortly after

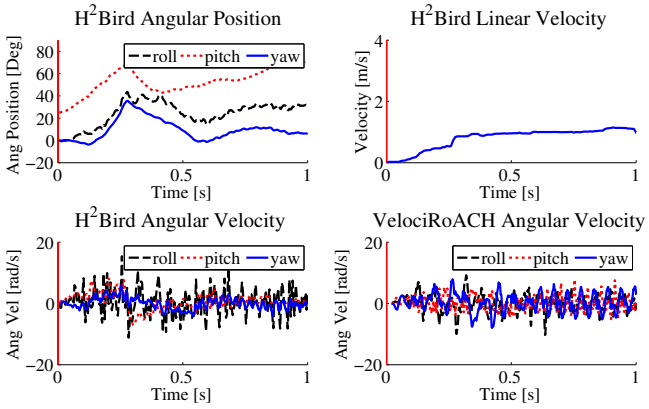

Fig. 5. Telemetry data at the start of running for a single launch trial.

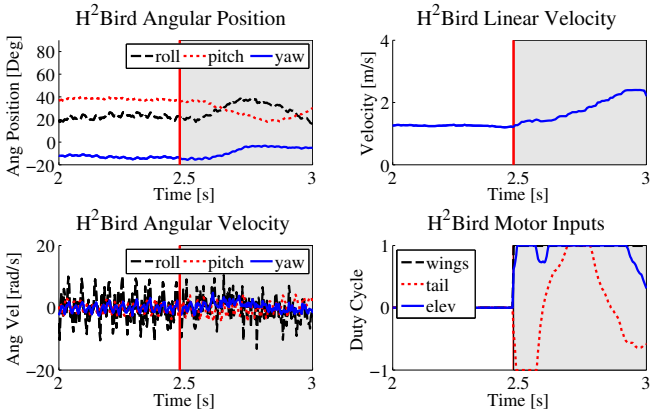

Fig. 6. Telemetry data around launch for a single launch trial. The red line indicates the launch point.

the steady state conditions are reached, and it detaches from the cradle.

A successful launch was defined as a launch in which the H²Bird did not touch the ground and ultimately traveled in an upwards direction after leaving the cradle. We did not have any requirements for the behavior of the VelociRoACH post-launch. We conducted trials at 16, 17, 18, and 20 Hz VelociRoACH stride frequencies in an effort to find the minimum stride frequency for successful launch. The H²Bird was free to pitch up in the cradle between 25 and 70 degrees from the horizontal. We did not constrain the pitching motion beyond the cradle properties previously mentioned. For each trial, we collected telemetry data from the H²Bird and VelociRoACH, and translational data from a Vicon[2] motion capture system.

The data collected for a typical trial are shown in Figures 5 and 6. The initial start-up transient is depicted in Figure 5. As shown in the figure, the H²Bird experiences an initial impulse increase in pitch angle of about 50 degrees, as well as roll oscillations of about 10 rad/s in magnitude. Both of these behaviors are due to the initial acceleration of the VelociRoACH. The behaviors 0.5 seconds before and after launch are in Figure 6. Right after launch, the H²Bird initially pitches down and there is an increase in velocity magnitude. The H²Bird angular controllers were on during the launch, which explains the changes in the duty cycle of the tail and elevator post-launch. Without these controllers, oscillations in pitch immediately after launch will cause the H²Bird to contact to the ground.

The results of the experiments are summarized in Figure 7, where the shaded region represents the area of initial conditions for which the wind tunnel data predicted failure, and the unshaded region represents the area of initial conditions for which the wind tunnel data predicted success. The circles represent experimental successes, and the triangles represent failures. The red triangles represent failures in the predicted success region.

We examined specific conditions of locomotion directly preceding and following the launch to determine why three launches succeeded in the wind tunnel predicted failure region and why four launches failed in the predicted success region.

There are several reasons for failure in the predicted success region of Figure 7. One failure mode that we observed is that the initial VelociRoACH acceleration could cause the H²Bird to rest in the stand in an unstable configuration. As shown on the right side of Figure 8, the failures in the predicted success region (indicated by red triangles) with less than 1.5 m/s takeoff velocity all had elevator input values less than 0.4. One trial at 1.38 m/s had a negative elevator input, which indicates that the H²Bird tried to pitch down after takeoff. These low elevator input values are caused by a takeoff angle greater than 45 degrees. The pitch controller regulates the pitch angle to 45 degrees post-takeoff, so the pitch controller in combination with high takeoff angles due to a poor resting state in the cradle can cause failure.

Another failure mode that we observed is that the H²Bird sometimes became caught on the front of the stand. This occurrence manifests itself in the form of a drop in pitch immediately following launching. The left side of Figure 8 shows that in some failure cases, the H²Bird lost a significant amount of pitch angle post-launch. The two red triangles at approximately 1.3 m/s and 1.4 m/s takeoff velocities experienced losses in pitch angle of -18 degrees and -27 degrees, respectively. This large dip in pitch angle could indicate that the back of the H²Bird hit the front of the stand as it released from the VelociRoACH.

Examining both the elevator input and the change in the pitch angle in Figure 9, we see that three out of the four failure cases in the predicted success region exhibited a combination of both losses in pitch angle post-launch and low elevator set points.

The final failure point, at 1.54 m/s launch velocity exhibited both the highest launch velocity and the largest increase in pitch angle post-launch. The combination of these two circumstances can cause the H²Bird to stall, experience a reduction in velocity and lift, and fall to the ground.

Although the wind tunnel can provide some idea as to the forces and moments that are experienced by the H²Bird in

[2]Vicon Motion Systems: http://www.vicon.com

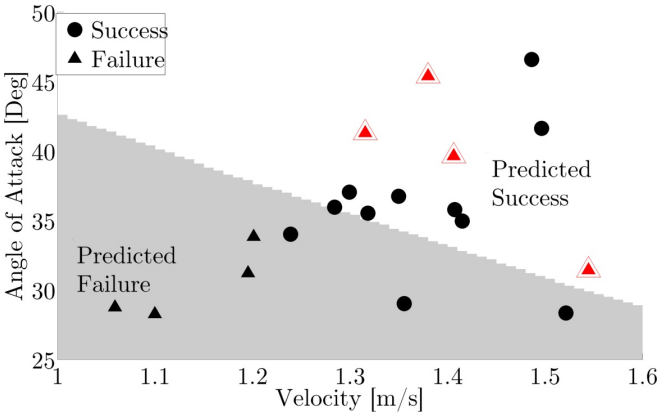

Fig. 7. Launch experiments for varied running speeds and launch angles. The shaded region represented the wind tunnel predicted failure area, and the unshaded region represents the predicted success area. The red double triangles represent failures in the predicted success region.

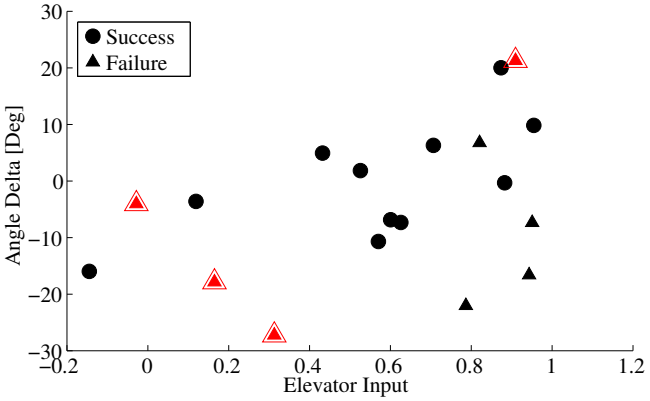

Fig. 9. The change in pitch angle vs. the elevator input for each trial. The red double triangles represent failures in the predicted success region.

free flight, the fact that the robot is rigidly mounted can cause some inconsistencies between what is happening in the wind tunnel and in unconstrained flight. These inconsistencies are detailed further in [16] and could explain the existence of successful trials in the predicted failure region.

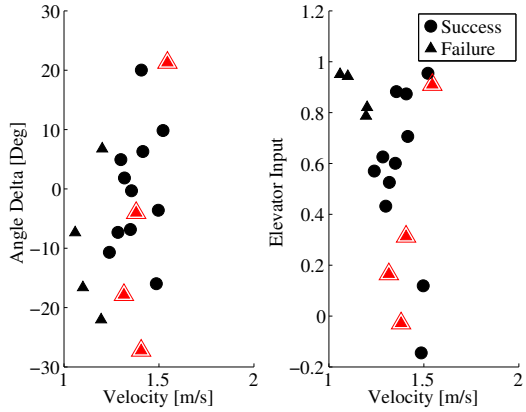

Fig. 8. The change in pitch angle 0.2 seconds post-launch for each tested velocity (left) and the elevator input at launch for each tested velocity (right). The red double triangles represent failures in the predicted success region.

B. Cooperative Running

To examine the effects of transporting the H^{2}Bird on top of the VelociRoACH, we conducted experiments running the VelociRoACH at a stride frequency of 17 Hz. For each trial, we started the robot from rest and recorded the angular velocities, linear velocity, battery voltage, motor duty cycles, and motor back electromotive force (back-EMF) for 5 seconds of running. We collected this data at 17 Hz stride frequency for the VelociRoACH running alone, running with an inertial mass sitting on top, running with the H^{2}Bird passively sitting in the cradle, and running with the H^{2}Bird with the yaw controller active and the wings flapping at 5 Hz. We chose a 5 Hz flap frequency because it was just low enough for the H^{2}Bird to remain stationary sitting on the stand. The inertial mass had approximately the same mass and inertia tensor as the H^{2}Bird.

The data for a typical trial are shown in Figure 10, with the case of the VelociRoACH alone, the VelociRoACH with the inertial mass, the passive H^{2}Bird case, and the active H^{2}Bird case from left to right. Examining the top row of plots, it is clear that the magnitude of the pitch velocity is reduced dramatically from the 'alone' case to the 'passive' and 'active' cases. The middle row of plots show that the presence of the H^{2}Bird induces a periodic spike in the motor torque for the VelociRoACH that is not as prominent in the 'inertial' case. The increase in the magnitude of the peaks in the pitch velocity and the motor torque from the 'inertial' case to the 'passive' case indicates that the running gait of the VelociRoACH is not only affected by the change in inertia provided by the H^{2}Bird, but the wings as well.

To determine the energetic penalty to the the VelociRoACH's running performance while carrying the H^{2}Bird, we computed the average power, $Power_i$, consumed by each motor over the 5 second trials at 17 Hz stride frequency, using the following equation:

$$Power_i = |DC_i| * V_{Batt} * \frac{(V_{Batt} - BEMF_i)}{R_i} \quad (2)$$

where $Power_i$ is the power input to motor i, DC_i is the duty cycle, $BEMF_i$ is the back-EMF, R_i is the motor resistance, and V_{Batt} is the battery voltage. The energetic data are presented in the right plot of Figure 12. Each point represents the average sum of the power going into each motor for the 6 trials for each experiment set, and the error bars are one standard deviation above and below the mean.

From Figure 12, the VelociRoACH motors consume more power for the passive and active trials with the H^{2}Bird on top, than they do for the VelociRoACH alone or with the inertial mass. This result is caused by the increased mass and higher center of gravity from the H^{2}Bird sitting on top of the VelociRoACH, as well as the drag provided by the wings. These additional forces require the motors to produce more torque as the feet contact the ground to keep the stride frequency at 17 Hz. Although carrying

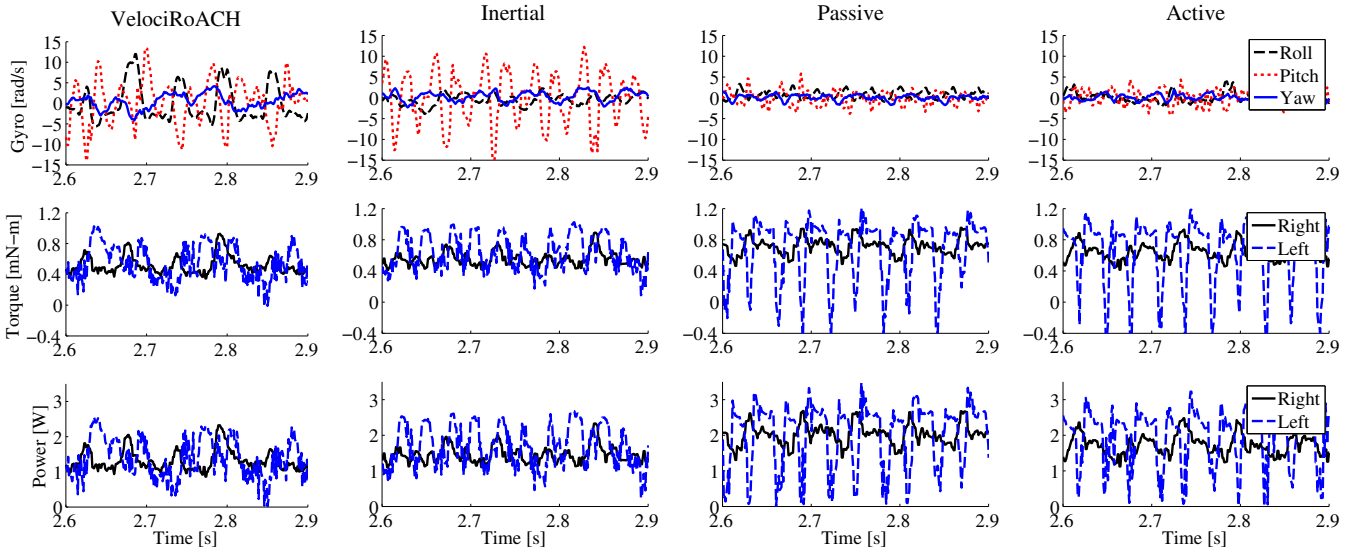

Fig. 10. Telemetry data for a single trial for the VelociRoACH running alone (left), running with an inertial mass equivalent to the H^{2}Bird, running with the passive H^{2}Bird, and running with the H^{2}Bird flapping at 5 Hz (right).

the H^{2}Bird is detrimental to the VelociRoACH in terms of power consumption, there are several benefits.

One benefit comes in the form of the angular velocities of the VelociRoACH as it runs. Figure 11 depicts the effect of the H^{2}Bird on the variance of the roll and pitch velocities experienced during running. Each point represents the mean variance in roll (left) and pitch (right) velocities for the four cases over 6 trials, and the error bars are one standard deviation above and below the mean. The VelociRoACH experienced a 91.1 percent reduction in the roll velocity variance simply by placing the H^{2}Bird in the stand, and a 95.0 percent reduction in the variance for the active H^{2}Bird. For pitch velocity variance, the VelociRoACH experienced an 80.0 percent reduction for the passive H^{2}Bird, and a 90.5 percent reduction for the active case.

While the active H^{2}Bird case had little benefit in terms of rotational damping over the passive case, and requires more total energy overall for locomotion, the benefit to the VelociRoACH comes in the form of running speed. Figure 12 shows the change in the average running velocity for each experimental case with the error bars representing one standard deviation above and below the mean of the 6 trials. The passive H^{2}Bird case results in a 8.4 percent decrease in average running velocity at steady state. This reduction is caused by the added drag force from the wings of the H^{2}Bird. By actively flapping the wings at 5 Hz, however, we measured a 12.7 percent increase in running velocity. The flapping provides a forward thrust force to counteract the drag force caused by the wings. The lift provided by the wings can reduce the ground contact forces as the VelociRoACH runs, reducing the torque required by the motors and enabling faster running.

All of the aforementioned benefits and detriments are summarized in Table I. Positive percentages indicate an increase in a particular measure over the VelociRoACH alone case, while negative percentages indicate a decrease.

We calculated the cost of transport for the H^{2}Bird in flight, for the VelociRoACH running alone, and for both cooperative cases according to the following equation:

$$COT = \frac{P}{mgv} = \frac{W}{mgd} \tag{3}$$

where P is average power consumed, m is mass, g is gravity, v is velocity, W is work, and d is distance. The calculated cost of transport for the VelociRoACH alone, the H^{2}Bird alone, and our two cooperative cases are in Table II. Placing the H^{2}Bird on top of the VelociRoACH decreases the cost of transport of the VelociRoACH by approximately 16 percent. This decrease in the cost of transport would be useful in a situation where the VelociRoACH and the H^{2}Bird had to both reach a point 80 meters away and the H^{2}Bird had to fly 20 meters in the air, where the VelociRoACH cannot reach. In one case, both robots travel the 80 meters separately, and then the H^{2}Bird continues the last 20 meters. In a second case, the VelociRoACH carries the H^{2}Bird for the first 80 meters, then the H^{2}Bird is launched and flies 20 meters. The second case consumes 25 percent less energy than the first. In situations such as these, cooperative locomotion would be more efficient than independent locomotion.

V. CONCLUSIONS

We have demonstrated a method for launching a flapping-winged MAV, the H^{2}Bird, using a legged hexapod, the VelociRoACH. We found that it is possible to reliably launch the H^{2}Bird from atop the VelociRoACH for successful flight, provided the legged robot reaches an appropriate minimum velocity of 1.2 m/s. A failure mode for velocities greater than this minimum is improper positioning in the carrying cradle as a result of pitch velocity impulses as the VelociRoACH initially accelerates to run. Additionally,

Data	Passive [% Change]	Active [% Change]
Average Power	+24.5	+18.1
Roll Velocity Variance	-91.1	-95.0
Pitch Velocity Variance	-80.0	-90.5
Yaw Velocity Variance	-25.3	-41.5
Average Velocity	-8.4	+12.7

TABLE I

TABLE OF PERCENT INCREASES AND DECREASES OF MEASURED DATA FOR THE ACTIVE AND PASSIVE H^{2}BIRD CASES OVER THE CASE OF THE VELOCIROACH RUNNING BY ITSELF.

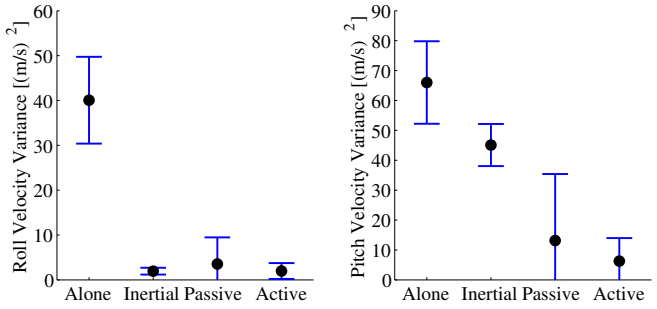

Fig. 11. Roll velocity variance (left) and pitch velocity variance (right) for the VelociRoACH alone, with inertial mass, with passive H^{2}Bird, and with active H^{2}Bird.

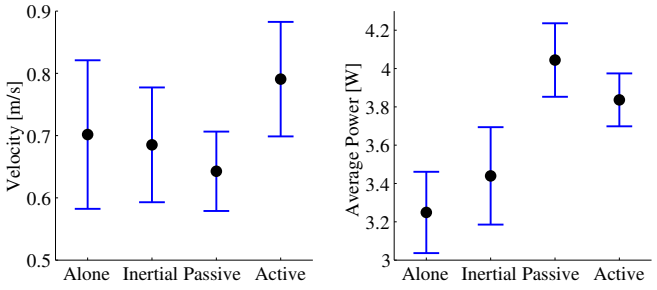

Fig. 12. Average running velocities (left) and average power consumed (right) at steady state for VelociRoACH alone, with inertial mass, with passive H^{2}Bird, and with active H^{2}Bird.

	VelociRoACH	H^{2}Bird	Passive	Active
Cost of Transport	8.1	10.1	6.8	6.6

TABLE II

TABLE OF COST OF TRANSPORT FOR THE VELOCIROACH ALONE, THE H^{2}BIRD ALONE, AND THE ACTIVE AND PASSIVE COOPERATIVE CASES.

the H^{2}Bird catching on the stand can cause a downward pitch immediately after launch that can cause the launch to fail.

Although the H^{2}Bird causes the VelociRoACH motors to consume approximately 18.1 to 24.5 percent more power, we found that the H^{2}Bird can have some beneficial effects on the running performance of the VelociRoACH. Just by simply resting on top of the VelociRoACH, the H^{2}Bird can reduce the variance of the roll and pitch velocities by about 80 and 90 percent, respectively. This pitch and roll damping can allow the legged robot to run more stably. Although the H^{2}Bird reduces the average running velocity at 17 Hz stride frequency by 8.4 percent, by flapping the wings at 5 Hz, the average velocity can be increased by 12.7 percent. We make no claims about the efficiency of the running gait for the VelociRoACH by carrying the H^{2}Bird. There are better ways to provide rotational damping, but the ability to carry a robot with an advantageous mode of transportation with minimal losses is an important result.

We intend to further experiment with these cooperative behaviors to determine if we can actively predict ideal conditions for launch. This information will enable the VelociRoACH to autonomously command the H^{2}Bird to launch with no human intervention. The reductions in cost of transport through the use of cooperative robotics can also allow for increased utility of millirobotic platforms.

ACKNOWLEDGMENT

The authors thank Ethan Schaler and Andrew Pullin for photography and videography expertise, Duncan Haldane for assistance with the robotic coordination, and the Biomimetic Millisystems Laboratory at the University of California, Berkeley for their advice and support.

REFERENCES

[1] J. H. Brown, *Scaling in Biology*. Santa Fe, NM: Oxford University Press, 2000.

[2] F. E. Zajac, "Muscle and tendon: properties, models, scaling, and application to biomechanics and motor control," *Critical reviews in biomedical engineering*, vol. 17, no. 4, pp. 359–411, 1989.

[3] L. C. Rome, "Scaling of muscle fibres and locomotion," *Journal of Experimental Biology*, vol. 168, pp. 243–252, July 1992.

[4] U. Saranli, M. Buehler, and D. E. Koditschek, "Rhex: A simple and highly mobile hexapod robot," *Intl. Journal of Robotics Research*, vol. 20, pp. 616–631, 2001.

[5] M. Buehler, U. Saranli, D. Papadopoulos, and D. Koditschek, "Dynamic locomotion with four and six-legged robots," in *Int. Symp. Adaptive Motion of Animals and Machines*, 2000.

[6] R. Full, K. Autumn, J. Chung, and A. Ahn, "Rapid negotiation of rough terrain by the death-head cockroach," *American Zoologist*, vol. 38, no. 81A, 1998.

[7] U. Pesavento and Z. Wang, "Flapping wing flight can save aerodynamic power compared to steady flight," *Physical Review Letters*, vol. 103, p. 118102, Sep 2009.

[8] A. Kossett and N. Papanikolopoulos, "A robust miniature robot design for land/air hybrid locomotion." in *Intl. Conf. on Robotics and Automation*. IEEE, 2011, pp. 4595–4600.

[9] A. Kalantari and M. Spenko, "Design and experimental validation of hytaq, a hybrid terrestrial and aerial quadrotor." in *Intl. Conf. on Robotics and Automation*. IEEE, 2013, pp. 4445–4450.

[10] K. Peterson and R. Fearing, "Experimental dynamics of wing assisted running for a bipedal ornithopter." in *Intl. Conf. on Intelligent Robotics and Systems*, 2011.

[11] R. Bachmann, F. Boria, R. Vaidyanathan, P. Ifju, and R. Quinn, "A biologically inspired micro-vehicle capable of aerial and terrestrial locomotion," *Mechanism and Machine Theory*, vol. 44, no. 3, pp. 513 – 526, 2009, special Issue on Bio-Inspired Mechanism Engineering.

[12] K. Peterson, P. Birkmeyer, R. Dudley, and R. Fearing, "A wing-assisted running robot and implications for avian flight evolution," *Bioinspiration and Biomimetics*, vol. 6, no. 4, p. 118102, 2011.

[13] D. Haldane, K. Peterson, F. G. Bermudez, and R. Fearing, "Animal-inspired design and aerodynamic stabilization of a hexapedal millirobot." in *Intl. Conf. on Robotics and Automation*, May 2013.

[14] R. Julian, C. Rose, H. Hu, and R. Fearing, "Cooperative control and modeling for narrow passage traversal with an ornithopter MAV and lightweight ground station," in *Intl. Conf. on Autonomous Agents and Multi-Agent Systems, AAMAS*, May 2013, pp. 103–110.

[15] A. Pullin, N. Kohut, D. Zarrouk, and R. Fearing, "Dynamic turning of 13 cm robot comparing tail and differential drive." in *Intl. Conf. on Robotics and Automation*. IEEE, 2012, pp. 5086–5093.

[16] C. Rose and R. Fearing, "Comparison of ornithopter wind tunnel force measurements with free flight," in *Intl. Conf. on Robotics and Automation*. IEEE, 2014.